Original citation:

Jia, Dagong, Zhang, Yulong, Li, Shuai, Xu, Tianhua, Zhang, Hongxia and Zhang, Yimo. (2015) Combined denoising filter for fringe pattern in electronic speckle shearing pattern interferometry. Optical Engineering, 54 (4). 043105.

Permanent WRAP URL:

http://wrap.warwick.ac.uk/93988

Publisher's statement:

Citation format:

Jia, Dagong, Zhang, Yulong, Li, Shuai, Xu, Tianhua, Zhang, Hongxia and Zhang, Yimo. Combined denoising filter for fringe pattern in electronic speckle shearing pattern interferometry. Optical Engineering, 54 (4). 043105. 2015.

DOI abstract link format:

http://dx.doi.org/10.1117/1.OE.54.4.043105

Combined denoising filter for fringe pattern in electronic speckle shearing pattern interferometry

Jia Dagong[a,*], Zhang Yulong[a], Li Shuai[a], Xu Tianhua[b], Zhang Hongxia[a], Zhang Yimo[a]

a. Tianjin University, College of Precision Instrument and Opto-electronics Engineering, Ministry of Education, Key Laboratory of Opto-electronics Information Technology, and Key Laboratory of MOEMS, Tianjin 300072, China

b. University College London, Department of Electronic and Electrical Engineering, Torrington Place, London WC1E 7JE, United Kingdom

*Corresponding author: dagongjia@tju.edu.cn

Abstract: We propose an effective image denoising filter, which combines an improved spin filter (ISF) and wave atoms thresholding (WA), to remove the noise of fringe patterns in electronic speckle shearing pattern interferometry (ESSPI). The WA is firstly employed to denoise the fringe to save the processing time, and then the ISF is further used to remove noise of the denoised image using WA to obtain a better denoising performance. The performance of our proposed approach is evaluated by using both numerically -simulated and experimental fringes. At the same time, three figures of merit for denoised fringe are also calculated to quantify the performance of CF. The denoised results produced by improved spin filting (ISF) , wave atoms thresholding (WA), and bilateral filtering(BF) are compared. The comparisons shows that our proposed method can effectively filter off the noise and an improvement of 12s in processing time and 0.3 in SI value with respect toISF is obtained.

Index Terms: electronic speckle shearing pattern interferometry (ESSPI), combined denoising filter (CF), improved spin filtering (ISF), wave atoms thresholding (WA)

1. Introduction

Electronic speckle-shearing pattern interferometry (ESSPI) can provide contactless, highly sensitive, and full-field measurements, and has been widely used in both academic researches and engineering applications [1]. However, ESSPI interferograms contain a high level of residual speckle noise due to random interference among the coherent returns [2], which makes the phase-information-extract more difficult. Therefore, the speckle noise reduction is a critical but challenging subject to obtain the accurate phase distribution from the ESSPI interferograms.

Many techniques have been proposed for fringe pattern denoising, such as the bilateral filtering (BF) [3], the spin filter [4], the oriented partial-differential equations [5], the wavelet transform [6], the wave-atom thresholding (WA) [7,8], and so on. The BF is a nonlinear adaptive filter which takes a weighted sum of the pixels in a local neighborhood, and the weights depend on both the spatial distance and intensity distance. Therefore, this method performs edge-preserving smoothing, but it has a tendency to over-smooth

[9].Both the spin filter and the oriented partial-differential equations are the oriented filtering which has been demonstrated to be a powerful tool for denoising fringe patterns in ESSPI [7-9, 10-11]. However, the key point of these methods relies on an accurate estimation of fringe orientation, which is difficult to determine due to the noise in the image. The wavelet transform is an effective algorithm to remove the noise in the frequency domain, but it is not to be very effective at image edges [12]. WA has been proven that it can effectively filter off the noise in the ESSPI interferograms, but the drawback is that the performance lies on an appropriate threshold. In order to preserve the details while removing noise, an ISF [13] has been proposed in our previous work which is an effective filter to remove noise for EESPI images, however, more iterations are required to achieve the best denoised results.

Meanwhile, some joint denosing algorithms are presented to remove noise for image, such as Bilateral Filtering and Dua-l Tree Complex Wavelet [14], dual tree complex wavelet and wave atoms [15], bilateral filter and Gaussian scale mixtures in shiftable complex directional pyramid domain [9] and wave atom, curvelet and wavelet transform [16]. Compared to the single denosing approaches, it is demonstrated that these denoising algorithms can efficiently preserve edges while denosing noise. In this paper, a new joint denosing approach which takes advantage of the ISF and WA for removing the noise of fringes in the ESSPI has been proposed to overcome the drawbacks of the improved spin filtering we have previously presented. The WA with regular threshold is firstly employed to remove noise of interferograms and the ISF is used to further denose the processed image in only one iteration.

The rest of this paper is organized as follows. In Section 2, the ISF is briefly discussed. Section 3 introduces the WA and discusses the effect of threshold on this algorithm. In section 4, CF is employed over the numerical simulated fringe and the experimentally obtained image of ESSPI. Compared to several relevant denoising algorithms, the performance of the presented denoising algorithm is discussed. Finally, a brief conclusion is given in Section 5.

2. Improved spin filter

The ISF is a denoising method in the spatial domain which removes the noise along the fringe orientation in the fuzzy directional window instead of the directional window [13]. So this denoising algorithm avoids accurately estimating the tangent orientation of fringe and issuitable for the fringe pattern in ESSPI. In the following content, we will shortly summarize the ISF.

First of all, four windows of n x n (e.g., 7 x 7) pixels with its center on the current point, x(i,j) ,are considered, as shown in Fig.1. Within the each window, a directional window of 3 x 7 is defined to remove noise. There are four types of directional window, orienting at 0, 90, 45 and 135 degrees, for x(i,j), where all the pixels are centrosymmetric around current point x(i,j). In order to contain all the tangent directions of x(i,j) within the defined window and to avoid increasing the number of picels off- tangent-directions, the directional window sizes should be 1/4 of fringe pattern width according to ref. [13]. Therefore, the window sizes are all defined as 3×n for 5×5、7×7、9×9 and 11×11 pixels windows, while for 13×13、15×15 and 17×17 pixels windows, the size 5× n will be better. Generally, when the square window size is larger than 17 ×17 or smaller than 5×5 pixels, there is no more advantages for this filter.

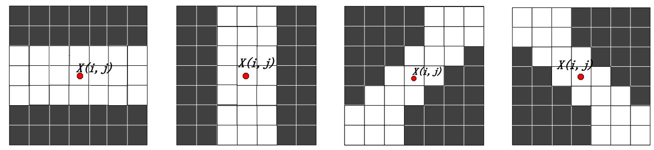

Fig.1.Pixels distribution of four directional windows of 7×7 pixels window

In a second step the average gray level A_{ij}^{d} and local variance σ^{2d}_{ij} of the current point x (i,j) will be calculated for four windows:

$$A_{ij}{}^{d} = \frac{1}{mn}\sum_{k=1}^{m}\sum_{l=1}^{n} I_{kl}^{d} \tag{1}$$

$$\sigma^{2}{}_{ij}{}^{d} = \frac{\sum_{k=1}^{m}\sum_{l=1}^{n}(I_{kl}{}^{d} - A_{ij}^{d})^{2}}{mn} \tag{2}$$

where *ij* denotes the position of x(i,j), *d* denotes the *d* th directional window, and I_{kl}^{d} denotes the gray level of *k*th row and *l*th column of each $m \times n$ directional window.

In the third step, since the varying gradient of the neighboring gray level is minimum along the tangent of the fringe and $\sigma^{2}{}_{ij}{}^{d}$ is the variance of gray level in the *d* th directional window [17], the directional window with the minimum variance $\sigma^{2}{}_{ij}{}^{d}$ is known as a window containing the fringe tangent direction. Thus this directional window can be defined as:

$$D = dir(\min(\sigma^{2^{d}}{}_{ij}))$$

Finally, the filtering action will be implemented in the *D*th directional window. The filter output $\hat{I}_{ij}$ can be calculated as follows:

$$\hat{I}_{ij} = \frac{\sum_{k=1}^{m}\sum_{l=1}^{n} I_{kl}^{D}\omega_{kl}^{D}}{\sum_{k=1}^{m}\sum_{l=1}^{n}\omega_{kl}^{D}} \tag{3}$$

Where ω_{kl}^{D} is a weight of I_{kl}^{D}, and is defined as

$$\omega_{kl}^{D} = \exp\left[\frac{-(I_{ij} - I_{kl}^{D})^{2}}{2\min(\sigma_{ij}^{2d})}\right] \tag{4}$$

where I_{ij} is the gray level of the current point.

The ISF is finished by repeating the above process for every pixel over the whole field.

3. Wave-atom thresholding

The wave atoms, as a generalization of curvelets, were introduced by Demanet [18]. In 2007, Alejandro Federico, et al. used WA to remove the noise in DSPI and this denoising algorithm had an outstanding performance and a high efficiency [8]. Resembling the wavelet thresholding algorithm, the threshold value of the WA also influences the denosing results. Similar to the wavelet, the WA have two types of threshold, one is soft threshold, the other is hard threshold. The hard threshold is expressed as:

$$\hat{\omega}_{hard} = \begin{cases} \omega_{hard}, & |\omega_{hard}| \geq \lambda \\ 0, & |\omega_{hard}| < \lambda \end{cases} \tag{5}$$

Where λ is threshold, $\hat{\omega}$ is the estimated wave atom transforming coefficients and ω is the wave atom transforming coefficient .

The soft threshold can be given as:

$$\hat{\omega}_{soft} = \begin{cases} \mathrm{sgn}(\omega_{soft})(|\omega_{soft}| - \lambda), & |\omega_{soft}| \geq \lambda \\ 0, & |\omega_{soft}| < \lambda \end{cases} \tag{6}$$

Here sgn() is a symbol function.

As to the two thresholds, it is noted that the hard threshold approach can preserve local characteristics of image edge but generates ringing artifact and Gibbs phenomenon. The soft threshold can similarly obtain smoothing denoising results but can cause fuzzy edge distortion [19].After weighing the advantages and disadvantages of both approaches, preserving the detail information of fringe pattern is more important for the ESSPI. So the wave-atom transformation with the hard threshold is used to remove noise. In this paper, the threshold value was selected as 2.12δ , where δ is the standard deviation of the intensity of the fringe pattern, in accordance with the Ref. [8].

4. Experimental Results and Discussion

In order to overcome the drawback of the improved spin filter, the WA with hard threshold is introduced to denoise the fringe pattern combining with the ISF in ESSPI. The proposed denoising approach comprises two steps. In the first step, WA is used to denoise the fringe in order to save the computing time and preserve the detailed information of images. In the second step, since the fringe patterns still contain some noise at the moment, the ISF is employed to reduce the noise of fringe pattern obtained from the first step. Generally, the best results can be obtained in one iteration using ISF. Thus it takes less time than only using the ISF to remove noise of the fringe patterns. To verify the correctness and validity of the proposed denoising algorithm, both numerical-simulated and experimental ESSPI fringes are selected to denoise.

Fig. 2 shows the simulated ESSPI fringe with noise and filtered results by the WA, ISF, BF and CF, respectively. Fig. 2(a) is a numerical–simulated noisy fringe pattern with resolution of 256×256 pixels and 256 gray levels. Fig. 2(b), Fig. 2(c), Fig. 2(d), and Fig. 2(e) show the denoised images withWA, CF, ISF

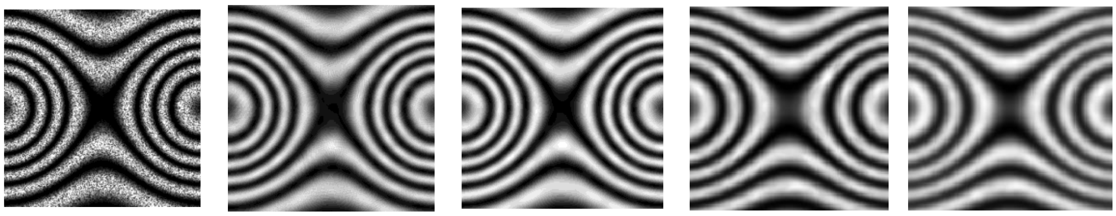

(a) **(b)** **(c)** **(d)** **(e)**

Fig.2.Simulated fringe patterns and its filtered results, (a) Noisy fringe pattern, (b) Filtered fringe pattern obtained by wave atoms thresholding, (c) Filtered fringe pattern by wave atoms thresholding combined with improved spin filter, (d) Filtered fringe pattern by improved spin filter，(e) Filtered fringe pattern by bilateral filtering

and BF, respectively. For this noisy fringe pattern, we choose the 3×7 directional windows for ISF according to fringe width of fringe pattern. From Fig. 2, it can be found that Fig. 2(b) and Fig. 2(c) are much clearer than Fig. 2(d); Fig. 2(e) and Fig. 2(b) are similar to Fig. 2(c) i.e. the denoised images using WA and CF show the better denoising of fringe pattern compared to the ISF and BF and the denoised image by the proposed algorithm is similar to that of WA. This can be seen visually as well as by calculating the fidelity *f* values for these images. The fidelity *f* is defined as [20]

$$f = 1 - \frac{\sum_{i=1}^{M}\sum_{j=1}^{N}\left[I_0(i,j) - I(i,j)\right]^2}{\sum_{i=1}^{M}\sum_{j=1}^{N}\left[I_0(i,j)\right]^2} \tag{7}$$

where $I_0(i,j)$ and $I(i,j)$ are the intensities of the noise-free image and the denoised image, respectively. A fidelity value close to 1 indicates that the filtered image is very similar to the noiseless one [21]. The calculation results are shown in the Fig.3. The comparison in the Fig. 3 shows that the value of *f* for Fig. 2(b) and Fig. 2(c) is lager than that of Fig. 2(d)and Fig. 2(e) and the denoised fringe using the combined method has the similar value to WA. So Fig. 2(c) shows the effectiveness of our proposed denoiding method.

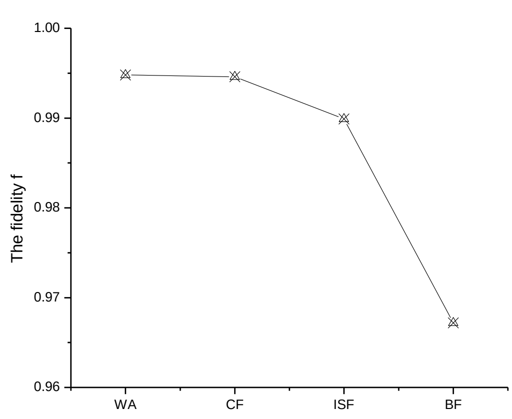

Fig.3 the value of f for the denoised fringe patterns using WA(wave atoms thresholding),CF(the combined filter), ISF(the improved spin filter)and BF(bilateral filtering)

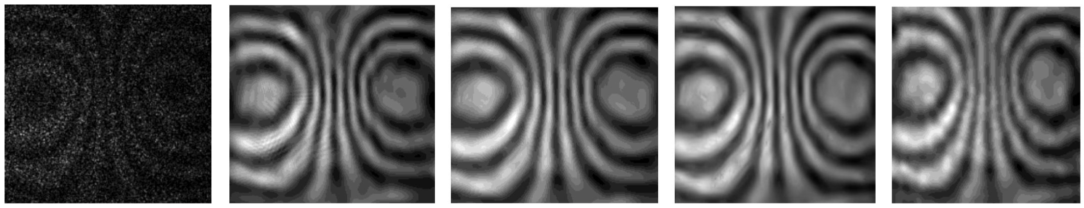

(a) (b) (c) (d) (e)

Fig.4.Experimental ESSPI fringe pattern and denoised results, (a) Initial fringe pattern, (b) Filtered fringe pattern obtained by wave atoms thresholding, (c) Filtered fringe pattern obtained by wave atoms thresholding combined with improved spin filter (d) Filtered fringe pattern by improved spin filter，(e) Filtered fringe pattern by bilateral filtering

In agreement with the simulation fringe, the experimental fringe pattern obtained by electric speckle shearing pattern interferometer [22] is also used to test the performance of CF. The denoised images are shown in Fig.4, where Fig.4 (a) shows the experimental fringe pattern. From Fig.4, it can be seen that Fig. 4(c) is much smoother than Fig. 4(b), Fig. 4(d) and Fig. 4(e) in visual perception. In the edge area the denoising effect of BF and WA is much worse than that of CF and ISF. Moreover the denoising image using WA contain the Gibbs phenomenon due to using the hard threshold algorithm. However Fig. 4(c) has no Gibbs phenomenon. The visual effect of Fig. 4(c) reveals that our proposed approach can improve the performance of WA with hard threshold in ESSPI. Those can also be verified by calculating the speckle index *SI* values and Peak signal-to-noise ratio (PSNR) values for these experimental images. The speckle index *SI* is given as [20]

$$SI = \frac{1}{N^2}\sum_{\mathrm{i,j=1}}^{\mathrm{n}}\frac{\sigma_{ij}}{\overline{I_{ij}}} \tag{8}$$

Where σ_{ij} and $\overline{I_{ij}}$ are the local standard deviation and the local mean over a 5×5 window, respectively, and *N* is the image horizontal and vertical dimensions in pixel. Generally the speckle index *SI* can be regarded as an average reciprocal of SNR [3]. Low values of the speckle index are considered as an indication of local smoothness.

Similar to f , The PSNR is also a parameter quantifying the denoising image , but PSNR is used to quantify the experimental image while f is used to quantify the simulation image. The Higher the PSNR is, the better the image details preserves. PSNR is expressed as [23]

$$PSNR = 10\lg\frac{255^2}{\frac{1}{MN}\sum_{i=1}^{M}\sum_{j=1}^{N}[I(\mathrm{i},j) - I_0(i,j)]^2} \tag{9}$$

Table.2 is the calculation results of SI, PSNR and the processing time in second for Fig. 3(b), Fig. 3(c), Fig.3(d), and Fig.3(e). As shown in the Table.1, the values of SI for WA, CF , ISF and BF are0.0293, 0.0289, 0.0318and 0.0316, respectively. A comparison of SI value shows that the performance of CF is

Table 1 PSNR, SI and the processing time in second of experimental image using WA, CF, ISF and BF

Method	PSNR(dB)	*SI*	Time(s)
wave atoms thresholding (WA)	23.4413	0.0293	5
The combined filter(CF)	23.5147	0.0289	13
improved spin filter (ISF)	23.7551	0.0318	25
bilateral filtering(BF)	23.4693	0.0316	11.2

better than that of others. Also, it shows that the joint denosing approach is a more effective denoisng algorithm for the fringe pattern in ESSPI. But a comparison of PNSR value shows that the value of PNSR for denoised fringe of CF is less than that of ISF and larger than that of WA and BF. So the ability of preserving the detail of CF is worse than that of ISF and a degradation of 0.2dB in PSNR value is obtained. The result may attribute to the fact the noise in the fringe is introduced by many factors, such as the the environmental vibration, the image acquisition systems and so on. In addition, in order to further evaluate the performance of our proposed approach, the processing time of algorithm is recorded and listed in the table 1. Compared to the processing time of ISF, an improvement of 12s is obtained when the noisy fringe pattern is denoised using CF. Therefore the execution time can be reduced and the drawback of ISF is overcome by using our proposed approach.

5. Conclusion

We propose a joint denoising method based on WA and ISF, for removing the noise of fringe in ESSPI. This algorithm first use the WA for the nosiy fringe patterns, then ISF with one iteration is employed to filter the denoised image using theWA. The performance of this joint method was evaluated in both numerical-simulated and experimental fringe patterns, respectively. The denoised results are compared to WA, ISF and BF. Moreover, three figure of merits, *f*, *SI* and *PSNR*, were calculated to verify our proposed method. It is shown from the calculation results and denoised image that the joint denoising method is an efficient and effective filter for the fringe pattern in ESSPI, which reduces the processing time compared to the ISF and has no Gibbs phenomenon compared with WA. However, regarding the detail protecting, the value of PSNR for CF is less than that of ISF, i.e. the performance of CF is worse than that of ISF. The improvement of ability to preserve the detail of CF will be the focus of our future work.

Acknowledgements

This work was supported by the National Basic Research Program of China 973 Program (No. 2014CB340103), Project of international cooperation and exchange NSFC-RFBR (No. 61111120099), Project of the National Natural Science Foundation of China (Grant No. 61377077). The authors would like to thank the editor and the anonymous reviewers for their constructive and helpful comments.

References

[1] N. K. Mohan and P. K. Rastogi, “Recent developments in digital speckle pattern interferometry,” Opt. Lasers Eng. 40, 439–445(2003).

[2] Saba Mirza, Rajesh Kumar, Chandra Shakher, "Study of various preprocessing schemes and wavelet filters for speckle noise reduction in digital speckle pattern interferometric fringes," Opt. Eng. 44, 045603-6(2005).

[3] Ruiz P D, Kaufmann G H. Evaluation of a scale-space filter for speckle noise reduction in electronic speckle pattern interferometry [J]. Optical Engineering, 1998, 37(8): 2395-2401.

[4] Yu Q, Liu X, Andresen K. New spin filters for interferometric fringe patterns and grating patterns [J]. Applied optics, 1994, 33(17): 3705-3711.

[5] Tang C, Han L, Ren H, et al. Second-order oriented partial-differential equations for denoising in electronic-speckle-pattern interferometry fringes [J]. Optics letters, 2008, 33(19): 2179-2181.

[6] Liu Z, Jing C, Zhang Y. Study of combined filter based on wavelet transform to denoise stripe images of electronic speckle shearography pattern interferometry [C]. Proceeding of SPIE, 2011, vol. 8200: 82000-1-82000-10.

[7] Demanet L, Ying L. Wave atoms and sparsity of oscillatory patterns [J]. Applied and Computational Harmonic Analysis, 2007, 23(3): 368-387.

[8] Federico A, Kaufmann G H. Denoising in digital speckle pattern interferometry using wave atoms [J]. Optics letters, 2007, 32(10): 1232-1234.

[9] Yang H Y, Wang X Y, Qu T X, et al. Image denoising using bilateral filter and Gaussian scale mixtures in shiftable complex directional pyramid domain [J]. Computers & Electrical Engineering, 2011, 37(5): 656-668.

[10] Wang H, Kemao Q. Comparative analysis on some spatial-domain filters for fringe pattern denoising [J]. Applied optics, 2011, 50(12): 1687-1696.

[11] Tang C, Gao T, Yan S, et al. The oriented spatial filter masks for electronic speckle pattern interferometry phase patterns [J]. Optics express, 2010, 18(9): 8942-8947.

[12] Escalante N, Villa J, de la Rosa I, et al. 2-D Continuous Wavelet Transform for ESPI phase-maps denoising [J]. Optics and Lasers in Engineering, 2013, 51(9): 1060-1065.

[13] Dagong J, Caibin M, IAqiang W. Denoising of electronic speckle interferogram based on improved spin filtering [J]. AetaOpticaSinica, 2012, 32(3): 0311001.

[14] CAO J, ZHOU Z, TANG Y, et al. Image Denoising Algorithm Based on Bilateral Filtering and Dual-Tree Complex Wavelet [J]. Acta Photonica Sinica, 2010, 9: 037.

[15] Kun L J H S. Image diffusion filtering based on dual tree complex wavelet and wave atoms [J]. Acta Physica Sinica, 2011, 12: 032.

[16] Swami P D, Jain A. Image denoising by supervised adaptive fusion of decomposed images restored using wave atom, curvelet and wavelet transform [J]. Signal, Image and Video Processing, 2012: 1-17.

[17] Yu Q, Liu X, Andresen K. New spin filters for interferometric fringe patterns and grating patterns [J]. Applied optics, 1994, 33(17): 3705-3711.

[18] Demanet, L.: Curvelets, wave atoms, and wave equations, Ph.D. Thesis, Caltech, http://math.stanford.edu/~laurent/papers/ThesisDemanet.pdf.

[19] Gai S, Yang G, Wan M, et al. Denoising color images by reduced quaternion matrix singular value decomposition [J]. Multidimensional Systems and Signal Processing, 2013: 1-14.

[20] Shulev A A, Gotchev A, Foi A, et al. Threshold selection in transform-domain denoising of speckle pattern fringes[C]//Holography 2005: International Conference on Holography, Optical Recording, and Processing of Information. International Society for Optics and Photonics, 2006: 625220-1-625220-7.

[21] Bernini M B, Galizzi G E, Federico A, et al. Evaluation of the 1D empirical mode decomposition method to smooth digital speckle pattern interferometry fringes [J]. Optics and lasers in engineering, 2007, 45(6): 723-729.

[22] Jia D, Yu C, Xu T, et al. Vibration analysis based on electronic stroboscopic speckle-shearing pattern interferometry [C]//International Conference of Optical Instrument and Technology. International Society for Optics and Photonics, 2008: 716014-716014-10.

[23] Ding K. Wavelets, curvelets and wave atoms for image denoising [C]//Image and Signal Processing (CISP), 2010 3rd International Congress on. IEEE, 2010, 2: 782-786.